4926 *Biochemistry* **2009,** *48,* 4926–4936
DOI: 10.1021/bi9004039

BIOCHEMISTRY
including biophysical chemistry & molecular biology
Article

Binding Regions of Outer Membrane Protein A in Complexes with the Periplasmic Chaperone Skp. A Site-Directed Fluorescence Study†

Jian Qu,‡ Susanne Behrens-Kneip,§ Otto Holst,‖ and Jörg H. Kleinschmidt*,‡

‡*Fachbereich Biologie, Universität Konstanz, Universitätsstraße 10, D-78464 Konstanz, Germany,* §*P26 Nosocomial Infections of the Elderly, Robert-Koch-Institute Nordufer 20, 13353 Berlin, Germany, and* ‖*Division of Structural Biochemistry, Research Center Borstel, Leibniz-Center for Medicine and Biosciences, Parkallee 4a/c, D-23845 Borstel, Germany*

Received March 9, 2009; Revised Manuscript Received April 16, 2009

Downloaded by UNIV KONSTANZ on November 5, 2009 | http://pubs.acs.org
Publication Date (Web): April 21, 2009 | doi: 10.1021/bi9004039

ABSTRACT: Periplasmic Skp facilitates folding and membrane insertion of many outer membrane proteins (OMPs) into the outer membrane of Gram-negative bacteria. We have examined the binding sites of outer membrane protein A (OmpA) from *Escherichia coli* in its complexes with the membrane protein chaperone Skp and with Skp and lipopolysaccharide (LPS) by site-directed fluorescence spectroscopy. Single-Trp OmpA mutants, W_n-OmpA, with tryptophan at position *n* in the polypeptide chain were isolated in the unfolded form in 8 M urea. In five $\beta_x W_n$-OmpA mutants, the tryptophan was located in β-strand *x*, in four $l_y W_n$-OmpA mutants, in outer loop *y*, and in three $t_z W_n$-OmpA mutants in turn *z* of the β-barrel transmembrane domain (*TMD*) of OmpA. *PD*W_{286}-OmpA contained tryptophan in the periplasmic domain (*PD*). After dilution of the denaturant urea in aqueous solution, spectra indicated a more hydrophobic environment of the tryptophans in $\beta_x W_n$ mutants in comparison to $l_y W_n$-OmpA and $t_z W_n$-OmpA, indicating that the loops and turns form the surface of hydrophobically collapsed OmpA, while the strand regions are less exposed to water. Addition of Skp increased the fluorescence of all OmpA mutants except *PD*W_{286}-OmpA, demonstrating binding of Skp to the entire β-barrel domain but not to the *PD* of OmpA. Skp bound the *TMD* of OmpA asymmetrically, displaying much stronger interactions with strands β_1 to β_3 in the N-terminus than with strands β_5 to β_7 in the C-terminus. This asymmetry was not observed for the outer loops and the periplasmic turns of the *TMD* of OmpA. The fluorescence results demonstrated that all turns and loops l_1, l_2, and l_4 were as strongly bound to Skp as the N-terminal β-strands. Addition of five negatively charged LPS per one preformed Skp·W_n-OmpA complex released the C-terminal loops l_2, l_3, and l_4 of the *TMD* of OmpA from the complex, while its periplasmic turn regions remained bound to Skp. Our results demonstrate that interactions of Skp·OmpA complexes with LPS change the conformation of OmpA in the Skp complex for facilitated insertion and folding into membranes.

In recent years, several studies indicated that the assembly of outer membrane proteins (OMPs)[1] of Gram-negative bacteria is facilitated by molecular chaperones (*1*−*4*), which prevent misfolding in the periplasm (for a review, see ref *5*). Deletion of the genes of either the seventeen kDa protein, Skp, or the survival factor A, SurA, led to reduced concentrations of OMPs in the outer membrane (OM), while deletion of both was lethal (*6*, *7*). Skp is required for the formation of soluble periplasmic intermediates of OMPs, and double mutants deficient of Skp and the protease DegP did not grow at 37 °C on rich medium (*2*). How Skp interacts with unfolded OMPs in the periplasm is not well understood. In studies on the kinetics of insertion and folding of outer membrane protein A (OmpA) into preformed lipid bilayers, Skp facilitated folding of OmpA into negatively charged membranes and when lipopolysaccharide (LPS) was present (*8*).

A wide range of OMPs were shown to bind to Skp of *Escherichia coli* (141 residues, 15.7 kDa); see, e.g., reports on OmpF (*1*), maltoporin (LamB) (*9*), phosphoporin (PhoE) (*2*), and many others (*10*). Skp bound to OmpA at 3:1 stoichiometry (*8*). Later the crystal structures (*11*, *12*) and biochemical experiments (*13*) revealed that Skp is a homotrimer. Stable 1:1 complexes were reported for the Skp trimer and the OMPs OmpA, OmpG, and YaeT of *E. coli*, the autotransporter NalP of *Neisseria meningitidis*, and the major porin FomA of

†This work was supported by Grant KL1024/4-1/2 to J.H.K. from the Deutsche Forschungsgemeinschaft (DFG).

*Address correspondence to this author. Tel: +49-7531-882291. Fax: +49-7531-883183. E-mail: joerg.helmut.kleinschmidt@uni-konstanz.de.

[1]Abbreviations: DOPC, 1,2-dioleoyl-*sn*-glycero-3-phosphocholine; DTNB, 5,5′-dithiobis(2-nitrobenzoic acid); LPS, lipopolysaccharide; MTSSL, 1-oxy-2,2,5,5-tetramethylpyrroline-3-methyl methanethiosulfonate; OM, outer membrane; OMP, outer membrane protein; OmpA, outer membrane protein A; *PD*, periplasmic domain; TM, transmembrane; *TMD*, transmembrane domain; TMP, transmembrane protein; Skp, 17 kDa protein; TCEP, tris(2-carboxyethyl)phosphine hydrochloride; W_n-OmpA, single-tryptophan mutant of OmpA carrying tryptophan at position *n* in the polypeptide chain; W_nC_m-OmpA, single-tryptophan (at position *n*), single-cysteine (at position *m*) mutant of OmpA; wt-OmpA, wild-type OmpA.

 Published on Web 04/21/2009 © 2009 American Chemical Society

Fusobacterium nucleatum (*14*). The dissociation constants of these complexes were in the nanomolar range, indicating that they are stable. The crystal structure of the Skp trimer (*11*, *12*) is clamplike and resembles a jellyfish with six α-helical tentacles that define a central cavity and protrude about 60 Å from a *β*-barrel body, the association domain. The clamps present a large surface ideal for binding and protecting of unfolded proteins until they are transferred to the OM. Skp is a very basic protein (p*I* ~10.5), and positive charges cover the entire surface of the tentacle domain, in particular at the tips of the tentacles. The surface also contains hydrophobic patches inside the tentacle basket. OMP binding to Skp is pH-dependent and not observed when either Skp or OMPs are neutralized at very basic or at very acidic pH (*14*). Therefore, electrostatic interactions dominated complex formation (*14*). In the OmpA·Skp_3 complex, Skp_3 efficiently shielded the tryptophans of the transmembrane (TM) strands of wild-type (wt) OmpA against fluorescence quenching by aqueous acrylamide. The addition of LPS resulted in stronger tryptophan fluorescence quenching by acrylamide, indicating that shielding of the tryptophans against the aqueous space is reduced in the presence of LPS (*14*). A possible LPS binding site has been reported and is composed of the basic Skp amino acid residues K_{97} R_{107}, and R_{108} and located near the center of the tentacle helices on the outer surface of Skp. This site is conserved among different species (*12*).

Here, we used site-directed fluorescence spectroscopy to examine the interactions of unfolded OmpA from *E. coli* with both Skp and LPS on the level of individual amino acid residues within OmpA. We prepared a range of single-tryptophan mutants of OmpA (W_n-OmpA mutants; *n* indicates the position of the tryptophan in the polypeptide chain), in which tryptophan can be selectively excited to study the changes in its microenvironment upon interactions with its binding partners or upon folding. The residues that we replaced by tryptophan were chosen to determine whether Skp or LPS preferentially binds to either *β*-strand, *β*-turn, or outer space loop regions of OmpA. We determined the effect of denaturant dilution on the aqueous forms of these W_n-OmpA mutants and then examined their interactions in separate experiments first with Skp and then with LPS. We next investigated whether addition of LPS to preformed Skp·W_n-OmpA complexes alters the environment of tryptophan in W_n-OmpA mutants. We finally isolated five different single-tryptophan/single-cysteine mutants of OmpA (W_nC_m-OmpA mutants). These mutants were labeled with a fluorescence quencher at the cysteine. Intramolecular site-directed fluorescence quenching was used to examine whether OmpA adopts a partially folded structure in complexes with Skp and LPS.

Table 1: List of Plasmids and Proteins of Single-Trp and W_nC_m Mutants of OmpA

(A) Plasmids and Proteins of Single-Trp Mutants of OmpA

plasmid	vector	Trp position	products	source
pET1102	pTRC99A	7	β_1W_7	*16*
pET1115	pTRC99A	15	β_1W_{15}	*16*
pET187	pUC18	57	β_3W_{57}	*16*
pET186	pTRC99A	102	β_5W_{102}	*16*
pET1103	pTRC99A	143	β_7W_{143}	*16*
pET24	pET22b	24	l_1W_{24}	this work
pET67	pET22b	67	l_2W_{67}	this work
pET110	pET22b	110	l_3W_{110}	this work
pET153	pET22b	153	l_4W_{153}	this work
pET48	pET22b	48	t_1W_{48}	this work
pET91	pET22b	91	t_2W_{91}	this work
pET131	pET22b	131	t_3W_{131}	this work
pET263	pET22b	263	PDW_{263}	this work
pET185	pTRC99A			*16*
pET22b185	pET22b			this work

(B) Plasmids and Proteins of W_nC_m OmpA Mutants[a]

plasmid	vector	Trp position	Cys position*	products	source
pTB001dc	pTRC99A	7	43	W_7C_{43}	unpublished
pTB003rdc	pTRC99A	57	35	$W_{57}C_{35}$	unpublished
pTB004dc	pTRC99A	7	170	W_7C_{170}	unpublished
pTB005dc	pTRC99A	15	162	$W_{15}C_{162}$	unpublished
pTB008dc	pTRC99A	15	35	$W_{15}C_{35}$	unpublished

[a] The two native cysteines, Cys_{290} and Cys_{302}, of the periplasmic domain were replaced by alanine by site-directed mutagenesis.

MATERIALS AND METHODS

Materials. *E. coli* strain XL1-blue *recA1 endA1 gyrA96 thi-1 hsdR17 supE44 relA1 lac* [F′ *proAB lacI*^{q}*Z*Δ*M15* Tn10 (Tet^r)] (Stratagene) was used for plasmid manipulations; *E. coli* strain BL21(DE3) omp8 fhuA [F$^-$, *ompT hsdS*$_B$ (r_B^- m_B^-) *gal dcm* (DE3) Δ*lamB ompF*::Tn5 Δ*ompA* Δ*ompC* Δ*fhuA*] (*15*) was used for the expression of OmpA mutants. Plasmids and primers used are listed in Tables 1 and 2. All oligonucleotide primers were purchased from MWG Biotech AG (Germany).

Table 2: Oligonucleotide Primers for Site-Directed Mutagenesis and Plasmid Construction

plasmid	sequence of primers[a]
pET24	5′-CCATGACACTGGTTTC**TGG**AACAACAATGGCCCG-3′
pET67	5′-GCCGTACAAAGGCAGC**TGG**GAAAACGGTGCATAC-3′
pET110	5′-CGACACTAAATCCAAC**TGG**TACGGTAAAAACCACG-3′
pET153	5′-GGTGACGCACACACC**TGG**GGCACTCGTCCGGACAAC-3′
pET48	5′-GTTACCAGGTTAACCCGT**GG**GTTGGCTTTGAAATG-3′
pET91	5′-CAATCACTGACGAC**TG**GGACATCTACACTC-3′
pET131	5′-CGGTGTTGAGTACGCG**TGG**ACTCCTGAAATCGC-3′
pET263	5′-CAGTCTGTTGTTGATT**GG**CTGATCTCCAAAGGTATC-3′
pET22b185	5′-CGGCATATGGCTCCGAAAGATAACACCTG-3′
	5′-CTGCTCGAGTTAAGCCTGCGGCTGAGTTACA-3′

[a] A pair of complementary primers was used to create each mutant. Only the sequence of the sense strand is shown. Changes in the sequences are shown in boldface type. *Nde*I and *Xho*I cut site sequences are shown underlined. These cut sites were used for cloning pET22b185 into the vector pET22b (Novagen).

Downloaded by UNIV KONSTANZ on November 5, 2009 | http://pubs.acs.org
Publication Date (Web): April 21, 2009 | doi: 10.1021/bi9004039

Downloaded by UNIV KONSTANZ on November 5, 2009 | http://pubs.acs.org
Publication Date (Web): April 21, 2009 | doi: 10.1021/bi9004039

The spin-labeling reagent 1-oxy-2,2,5,5-tetramethylpyrroline-3-methyl methanethiosulfonate (MTSSL) was obtained from Reanal (Budapest, Hungary). Methyl-4-nitrobenzenesulfonate, 5,5′-dithiobis(2-nitrobenzoic acid) (DTNB), and tris (2-carboxyethyl)phosphine hydrochloride (TCEP) were purchased from Sigma-Aldrich (Germany). 1,2-Dioleoyl-*sn*-glycero-3-phosphocholine (DOPC) was purchased from Avanti Polar Lipids (Alabaster, AL).

Construction of a Plasmid To Express OmpA Mutants into Inclusion Bodies. The sequence of the gene encoding a proOmpA mutant, in which all tryptophan residues were replaced by phenylalanine, was amplified from plasmid pET185 (*16*) by polymerase chain reaction (PCR) with Pfu Ultra polymerase from Stratagene (Amsterdam, The Netherlands) using the primers listed in Table 2. In the forward primer, the signal sequence of *proompA* was removed. The PCR product was then cloned into the pET22b vector (Novagen) to obtain plasmid pET22b185.

Construction of the Plasmids of Single-Tryptophan Mutants. The eight new plasmids, prepared for this work, were based on plasmid pET22b185. Site-directed mutagenesis was performed using the QuickChange II kit (Stratagene) as described using the primers listed in Table 2. The resulting plasmids were isolated and verified by sequencing.

Expression and Purification of OmpA Mutants. For expression and purification, plasmids were transformed into *E. coli* BL21(DE3) strain (*15*). Cells were grown in 2 L of LB medium for 3 h. IPTG was then added to a final concentration of 0.1 mM. After 4−6 h of induction, cells were harvested by 30 min of centrifugation (1500*g*, 4 °C). The wet cell paste was resuspended in 40 mL of Tris buffer (20 mM Tris, 0.1% 2-ME, pH 8.0) using an ice/water cooling bath. Lysozyme was added to a concentration of 50 μg/mL, and the mixture was stirred for 30 min at room temperature and then sonified for 30 min using a Branson ultrasonifier W-450D (20% power, 50% pulse cycle) with a macrotip in an ice/water bath. Soluble proteins were removed by centrifugation at 3000*g* (4 °C, 30 min). The pellet was resuspended in 20 mL of 20 mM Tris buffer, pH 8.0, and 0.1% 2-ME, containing 8 M urea. An equal volume of 2-propanol was added, and the mixture was incubated at 55 °C for 30 min. The pellet was removed by centrifugation (5000*g*, 30 min, 25 °C). The supernatant was loaded onto a Q-sepharose FF column (Amersham), which was pre-equilibrated with buffer containing 4 M urea and 50% 2-propanol. A NaCl gradient (0−100 mM) was used to elute the OmpA mutants from the column.

The OmpA mutant plasmids constructed in previous work expressed OmpA mutants into the OM of *E. coli*. They are listed in Table 1 and were purified as reported (*17*).

MTSSL Spin-Labeling and S-Methylation of Single-Tryptophan/Single-Cysteine Mutants. The single-tryptophan/single-cysteine mutants of OmpA (W_nC_m mutants) were expressed into the OM and purified as described (*17*). S-Methylation was carried out using a modified procedure of Hunziker (*18*). A 5-fold molar excess of TCEP was added to denatured W_nC_m mutants in borate buffer (50 mM, 1 mM EDTA, pH 9.0) containing 8 M urea. After 30 min of incubation at room temperature, a 40-fold molar excess of methyl-4-nitrobenzenesulfonate in acetonitrile was added. The sample tube was incubated at 37 °C for 60 min. Unreacted methyl-4-nitrobenzenesulfonate was removed by extensive dialysis.

MTSSL spin-labeling was performed as published (*19*). About 10 mg of denatured OmpA mutant was diluted in 1 mL of 10 mM Tris buffer, pH 7.2, containing 8 M urea and 1 mM EDTA. Disulfide bonds that may form between W_nC_m OmpA mutants were reduced by reacting denatured OmpA with a 5-fold molar excess of TCEP for 30 min at room temperature. Subsequently, 90 μL of MTSSL in absolute ethanol was added to the reaction tube at a molar ratio of MTSSL/OmpA of 10. The mixture was reacted at least 12 h in the dark at room temperature. Excess MTSSL was removed by extensive dialysis.

To determine the degree of S-methylation and MTSSL spin-labeling, an aliquot of the solution was taken, and DTNB was added in a 10-fold molar excess followed by spectrophotometric determination of free thiol groups at 412 nm, using $\varepsilon_{412} = 13700\ M^{-1}\ cm^{-1}$ (*20*).

Purification of Skp. The Skp protein of *E. coli* was purified as described (*8*).

Purification of LPS. *E. coli* rough mutant F576 was cultivated as described previously (*21*), and its LPS (R2 core type, $M \approx 3900$ g/mol) was isolated as reported (*22*).

Fluorescence Spectroscopy. Fluorescence spectra were recorded as described previously (*8*) on a Spex Fluorolog-3 spectrofluorometer with double monochromators in the excitation and emission paths. For each experiment, three samples were prepared and spectra recorded at 25 °C. The excitation wavelength was 295 nm, and the bandwidths of the excitation and emission monochromators were 2.5 and 5 nm, respectively. The integration time was 0.05 s, and an increment of 0.5 nm was used to scan spectra in the range of 310−380 nm. Three scans were averaged. All experiments were performed in 10 mM Tris buffer at pH 8.0 and at 25 °C. The final concentrations were 1.15 μM OmpA mutant, 4.6 μM Skp, and 5.75 μM LPS. Fluorescence spectra were analyzed using IGOR Pro 6.0 (Wavemetrics, Oregon). Spectra were fitted to a log-normal distribution (*23*) to obtain the fluorescence intensities at 330 nm and the wavelengths of the fluorescence intensity maxima (λ_{max}).

Spectra Aquisition for Urea-Unfolded and for Aqueous OmpA Mutants. The unfolded OmpA mutant (10 μL) was diluted into 490 μL of Tris buffer (10 mM, pH 8.0) either in the presence or in the absence of 8 M urea, and its spectrum was recorded. The background spectrum of the buffer was subtracted.

Binding of Skp to OmpA Mutants. Skp (4.5 μL, 8 g/L) was added into 490 μL of Tris buffer (10 mM, pH 8.0), and the background spectrum was recorded. Ten microliters of the OmpA mutant (2 g/L) were then added to record the spectrum after 30 s of incubation.

Binding of LPS to OmpA Mutants. Ten microliters of unfolded OmpA mutants (57.5 μM) were diluted into 490 μL of Tris buffer (10 mM, pH 8.0), and spectra were recorded. After addition of 4.5 μL of LPS (2.5 g/L) and 30 s of incubation, spectra of LPS·OmpA mutant complexes were recorded. Background spectra in the absence of OmpA were subtracted.

Binding of LPS to OmpA·Skp Complexes. Skp (4.5 μL, 8 g/L) was added to 490 μL of Tris buffer (10 mM, pH 8.0), and the background spectrum was recorded. Ten microliters of OmpA mutant (2 g/L) and then 4.5 μL of LPS (2.5 g/L) were added. Spectra of the OmpA·Skp·LPS complexes were recorded after 30 s of incubation. The previously recorded background spectra were subtracted.

RESULTS

Folding of Single-Trp Mutants of OmpA. To explore which sites within OmpA are in contact with Skp or LPS upon

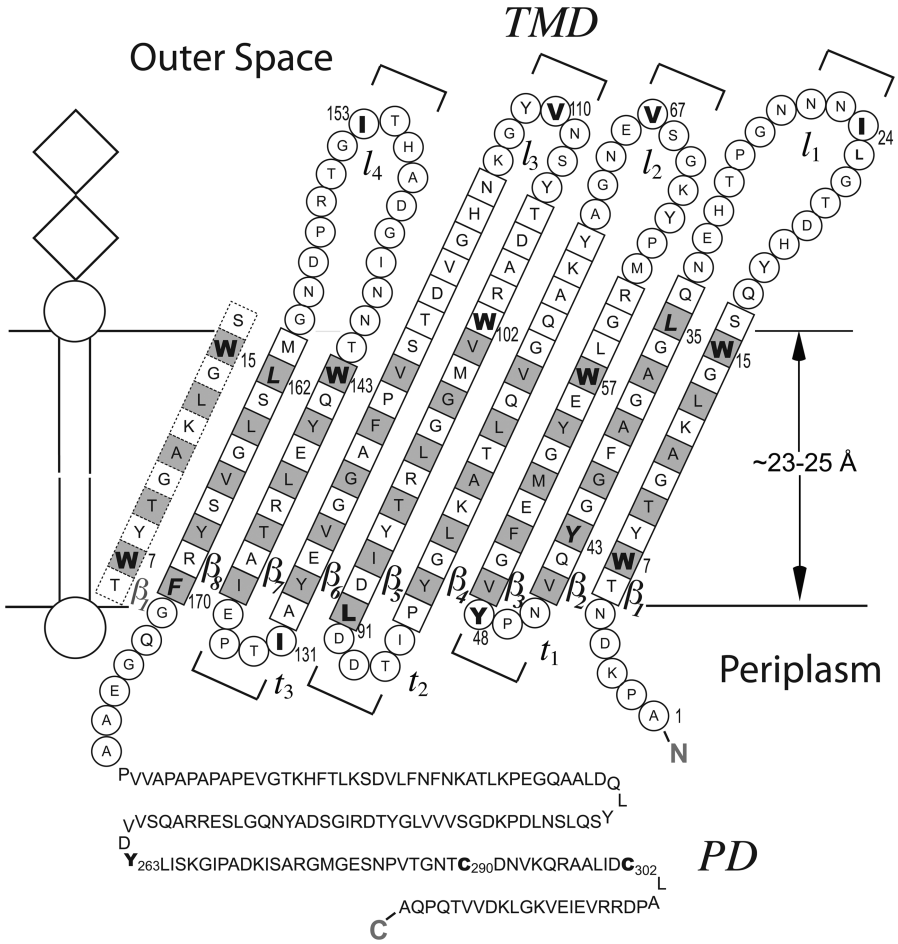

FIGURE 1: Transmembrane topology of wt-OmpA and sites selected to probe binding of Skp and LPS. β-Strand residues are indicated by squares and loop and turn residues by circles. Residues facing the hydrophobic lipid chains are indicated by a gray background. A plasmid containing an OmpA gene, in which the codons for the five native Ws were replaced by codons for phenylalanines (*16*), served as a template for site-directed mutagenesis. Residue positions selected for the preparation of single-tryptophan mutants of OmpA (W_n-OmpA) are shown in bold. In 13 different mutants, a single W was introduced at positions 7, 15, 24, 48, 57, 67, 91, 102, 110, 131, 143, 153, and 263 of the OmpA polypeptide chain. Residues replaced by cysteine (i.e., L_{35}, Y_{43}, L_{162}, and F_{170}) to obtain single-tryptophan, single-cysteine mutants (W_nC_m-OmpA) with W_n and C_m in proximity in neighboring β-strands are typeset in bold italic. The β-strands of OmpA are numbered starting from the N-terminus as $\beta_1-\beta_8$, the loops as l_1-l_4, and the turns as t_1-t_3.

Downloaded by UNIV KONSTANZ on November 5, 2009 | http://pubs.acs.org
Publication Date (Web): April 21, 2009 | doi: 10.1021/bi9004039

complex formation, we expressed and purified 13 different single-tryptophan mutants of OmpA. The expression systems were derived from a previously prepared plasmid encoding a tryptophan- (W-) free mutant of OmpA, in which all native Ws were replaced by phenylalanine (*16*). Figure 1 shows the topology of OmpA. In five single-W mutants of OmpA, designated β_xW_n, the W was located at position *n* of the polypeptide chain in strand β_x of the TM domain (*TMD*), *x* indicating the number of the strand starting from the N-terminus. These mutants were β_1W_7, β_1W_{15}, β_3W_{57}, β_5W_{102}, and β_7W_{143} OmpA (*16*). In four l_yW_n mutants, the single W was located in a *TMD*-loop l_y: l_1W_{24}, l_2W_{67}, l_3W_{110}, and l_4W_{153}. In three t_zW_n mutants, the W was introduced in *TMD*-turn t_z: t_1W_{48}, t_2W_{91}, and t_3W_{131}. In addition, a single-W mutant was prepared, containing the W in the periplasmic domain, *PD*, of OmpA: PDW_{263}.

All mutants were isolated in their unfolded forms in 8 M urea. Folding of the β_xW_n mutants was described previously (*16*, *24*). We confirmed insertion and folding of the new single-W mutants, l_yW_n, t_zW_n, and PDW_{263}, by reacting them with preformed lipid bilayers (small unilamellar vesicles, SUVs) of dioleoylphosphatidylcholine (DOPC). After incubation with DOPC bilayers, all mutants migrated at 30 kDa on SDS−polyacrylamide gels (Figure 2), indicating that they had folded. The 30 kDa form strictly corresponds to fully functional OmpA as described in previous studies; see ref *25* for a review. Unfolded fractions migrating at 35 kDa were minor.

Fluorescence Spectra of Single-Tryptophan Mutants in Unfolded, Aqueous, and Skp-Bound Form. We first recorded the fluorescence spectra of four W_n-OmpA mutants, β_1W_{15}, l_1W_{24}, t_1W_{48}, and PDW_{263}, in denatured (D) and in aqueous (AQ) forms after urea dilution (Figure 3). In 8 M urea, the spectra of all mutants had similar line shapes and intensities. The wavelengths of the fluorescence emission maxima, λ_{max}, were all at ~347 nm (Table 3). After urea dilution, slight decreases of the fluorescence intensities of β_1W_{15}, l_1W_{24}, and t_1W_{48} were observed (Figure 3), and the λ_{max}(AQ) of these three mutants were shifted to 340.6, 344.4, and 342.6 nm, respectively. The shift was smallest for l_1W_{24} OmpA with $\Delta\lambda_{max} \approx -2.5$ nm, followed by t_1W_{48} ($\Delta\lambda_{max} \approx -4.3$ nm) and β_1W_{15} ($\Delta\lambda_{max} \approx -6.4$ nm). This indicated that l_1W_{24} and t_1W_{48} were in less hydrophobic environment than β_1W_{15}. PDW_{263} displayed the strongest fluorescence changes, with strong quenching after urea dilution and a shift in the intensity maximum by $\Delta\lambda_{max} \approx -12$ nm to ~335 nm, suggesting the W is buried inside the periplasmic domain. The large differences between the fluorescence properties of Ws placed into the *TMD* and the W incorporated into the *PD*

Table 3: Fluorescence Intensities at 330 nm (F_{330}) and Wavelength of Fluorescence Emission Maxima (λ_{max})[a] of W_n-OmpA Mutants (F_{330} in Mcps; λ_{max} in nm)

W_n-OmpA	F_{330}(D)[b]	F_{330}(AQ)[c]	F_{330}(+LPS)[d]	F_{330}(+Skp)[e]	F_{330}(+Skp+LPS)[f]	λ_{max}(D)[b]	λ_{max}(AQ)[c]	λ_{max}(+LPS)[d]	λ_{max}(+Skp)[e]	λ_{max}(+Skp+LPS)[f]
β_1W_7	0.184	0.151	0.162	0.287	0.258	347.8	344.6	344.1	339.8	340.4
β_1W_{15}	0.193	0.214	0.219	0.438	0.381	347.0	340.6	340.2	336.3	336.8
l_1W_{24}	0.184	0.156	0.170	0.352	0.244	346.9	344.4	343.0	338.7	340.5
t_1W_{48}	0.183	0.174	0.180	0.353	0.322	346.9	342.6	342.7	337.9	338.1
β_3W_{57}	0.194	0.213	0.220	0.342	0.311	345.8	339.8	339.4	335.9	336.6
l_2W_{67}	0.191	0.187	0.194	0.371	0.257	346.9	343.9	343.5	338.2	340.8
t_2W_{91}	0.177	0.173	0.177	0.302	0.287	347.8	343.3	343.2	339.1	339.6
β_5W_{102}	0.195	0.201	0.205	0.314	0.297	346.5	339.7	339.4	336.9	337.2
l_3W_{110}	0.196	0.200	0.228	0.346	0.272	346.2	341.8	340.0	338.6	339.7
t_3W_{131}	0.190	0.178	0.181	0.370	0.294	346.5	342.2	342.4	337.4	338.4
β_7W_{143}	0.189	0.206	0.212	0.331	0.295	346.7	340.5	339.7	338.3	338.2
l_4W_{153}	0.178	0.148	0.158	0.306	0.197	347.1	344.3	343.7	339.2	342.0
PW_{263}	0.188	0.079	0.086	0.096	0.113	347.2	334.7	334.8	334.4	334.0

[a] λ_{max} was calculated by fitting the spectra to a log-normal distribution (*23*). [b] W_n-OmpA in 8 M urea. [c] W_n-OmpA in H_2O. [d] W_n-OmpA in the presence of a 5-fold molar excess of LPS. [e] W_n-OmpA in the presence of a 4-fold molar excess of Skp. [f] W_n-OmpA in the presence of a 4-fold molar excess of Skp and a 5-fold molar excess of LPS.

Downloaded by UNIV KONSTANZ on November 5, 2009 | http://pubs.acs.org
Publication Date (Web): April 21, 2009 | doi: 10.1021/bi9004039

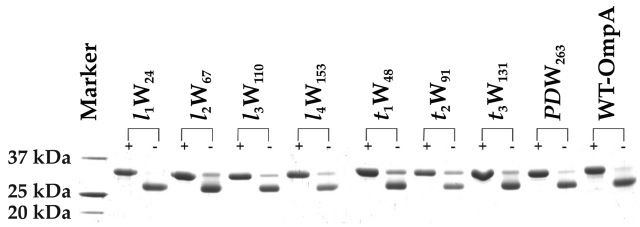

FIGURE 2: Folding of single-Trp mutants of OmpA into DOPC bilayers at 40 °C. SDS−PAGE demonstrates that the single-Trp mutants prepared in this study, namely, all l_yW_n and t_zW_n carrying the single tryptophan either in the outer loops or in the periplasmic turns, and PDW_{263} folded into lipid bilayers of DOPC (SUVs). Folded and unfolded wt-OmpA are shown for comparison. The samples were either boiled (+) or not (−) before loading them onto the gel. The 30 kDa form of OmpA was shown previously by spectroscopy (*16*, *17*, *34*, *35*), by phage inactivation assays (*36*), by proteolysis (*17*, *37*), and by single-channel conductivity measurements (*24*) to correspond to completely folded and functionally active OmpA.

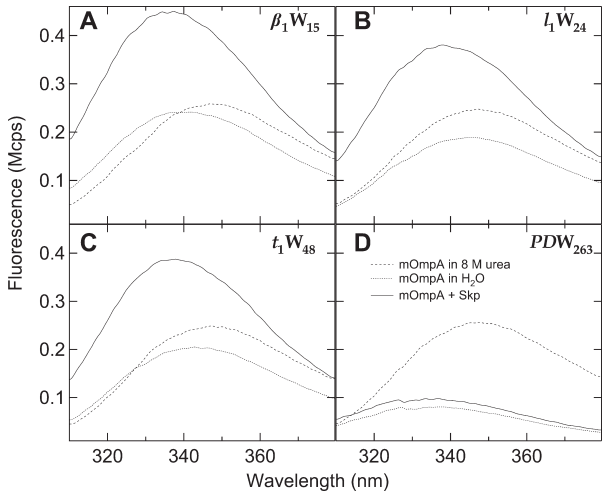

FIGURE 3: Fluorescence spectra of single-Trp mutants of OmpA in denatured form and after denaturant dilution in aqueous solution in the absence and presence of Skp. Fluorescence spectra of four representative single-Trp mutants of OmpA are shown: (A) β_1W_{15}, (B) l_1W_{24}, (C) t_1W_{48}, and (D) PDW_{263}. For each OmpA mutant, spectra were recorded in 8 M urea (- - -), in Tris buffer (10 mM, pH 8.0) (· · ·) after 50-fold dilution of urea, and in the presence of a 4-fold molar excess of Skp (—), The concentration of each OmpA mutant was 1.15 μM. Spectra were recorded at 25 °C.

suggested that the *PD* develops structure independently in aqueous solution, consistent with the hypothesis that the soluble *PD* already folds to its native conformation, while the *TMD* folds to an aqueous intermediate.

Upon Skp binding, the fluorescence intensities of l_1W_{24}, t_1W_{48}, and β_1W_{15} were strongly increased (Figure 3A−C), doubled at λ = 330 nm (F_{330}). The intensity maxima, λ_{max}(+Skp), of the Skp bound mutants were shifted by $\Delta\lambda_{max} \approx -4.3$ nm for β_1W_{15}, by $\Delta\lambda_{max} \approx -5.7$ nm for l_1W_{24}, and by $\Delta\lambda_{max} \approx -4.7$ nm for t_1W_{48} to 336.3, 338.7, and 337.9 nm, respectively (Table 3). In contrast, Skp affected the fluorescence of PDW_{263} only slightly (Figure 3D). F_{330} of PDW_{263} was increased by just 20%, and the shift $\Delta\lambda_{max}$ was only 0.4 nm (Table 3). The relatively minor change indicated little or no association of Skp with the *PD*, in agreement with previous observations (*14*). Most interestingly, these experiments indicated that the interactions of Skp with OmpA are not limited to the hydrophobic strand β_1. Skp binding to the polar loop l_1 and polar turn t_1 of the *TMD* of OmpA resulted in similar or even larger fluorescence changes.

Skp Binds Strands, Loops, and Turns of the Entire Unfolded Transmembrane Domain of OmpA. To investigate whether the results obtained for β_1W_{15}, l_1W_{24}, and t_1W_{48} are representative for the entire *TMD*, we recorded the fluorescence spectra of unfolded, aqueous, and Skp-bound forms of l_2W_{67}, l_3W_{110}, l_4W_{153}, t_2W_{67}, t_3W_{131}, β_1W_7, β_3W_{57}, β_5W_{102}, and β_7W_{143}. Figure 4 shows the emission λ_{max} of the spectra of the aqueous and Skp-bound forms of OmpA as a function of the position *n* of the single W in the polypeptide chain. For the aqueous forms (Figure 4A, open symbols), shifts of the emission maxima were strongest for the spectra of β_1W_{15}, β_3W_{57}, β_5W_{102}, and β_7W_{143} and were from λ_{max}(D) = ~346−348 nm to λ_{max}(AQ) ~340 nm; i.e., $\Delta\lambda_{max}$ ranged from −6 to −8 nm. This suggests that the β-strands are at the core of the water-collapsed *TMD*. The β_1W_7 mutant with W near the N-terminus was an exception among the mutants containing the W in the *TMD*. Its emission maximum (λ_{max}(AQ) = ~345 nm) displayed the smallest change, $\Delta\lambda_{max}$ = −3 nm compared to the denatured form (Figure 4, Table 3), suggesting it remains closer to the surface of the *TMD*. Similar to β_1W_7, only small shifts in λ_{max} were observed for l_1W_{24}, l_2W_{67}, l_4W_{153}, t_1W_{48}, and t_2W_{91} (λ_{max}(D) = ~346−348 nm was shifted to λ_{max}(AQ) = ~343−344 nm), indicating that loops and turns

Downloaded by UNIV KONSTANZ on November 5, 2009 | http://pubs.acs.org
Publication Date (Web): April 21, 2009 | doi: 10.1021/bi9004039

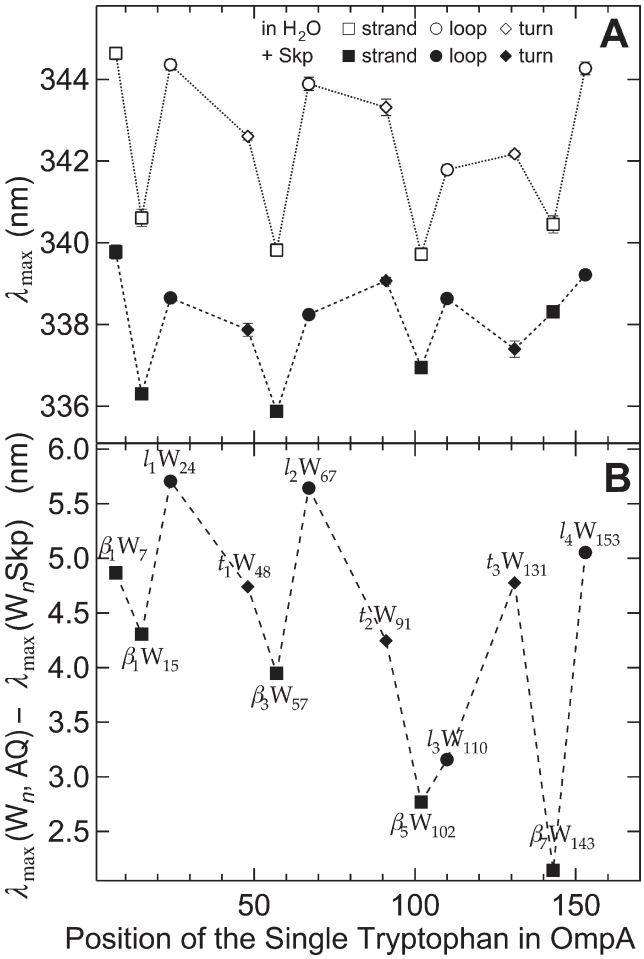

FIGURE 4: Fluorescence spectroscopy indicates tight binding of the entire transmembrane domain of OmpA to Skp. (A) The wavelengths of fluorescence emission maxima λ_{max} of single-Trp OmpA mutants (W_n-OmpA) are shown as a function of the position n of the inserted tryptophan for W_n-OmpA in aqueous solution (open symbols) and in the presence of Skp (filled symbols). For the β-strands β_x (□, ■), fluorescence maxima are mostly located at shorter wavelength, λ_{max}, than for outer loops, l_y (○, ●), and β-turns, t_z (◇, ◆). (B) The absolute difference of these emission maxima of the W_n-OmpA mutants in the absence and presence of Skp, $\lambda_{max}(W_n, AQ) - \lambda_{max}(W_n, Skp)$, indicates that the surface-exposed loops and turns of the aqueous form of OmpA are more strongly affected by Skp binding than tryptophans introduced in β-strands.

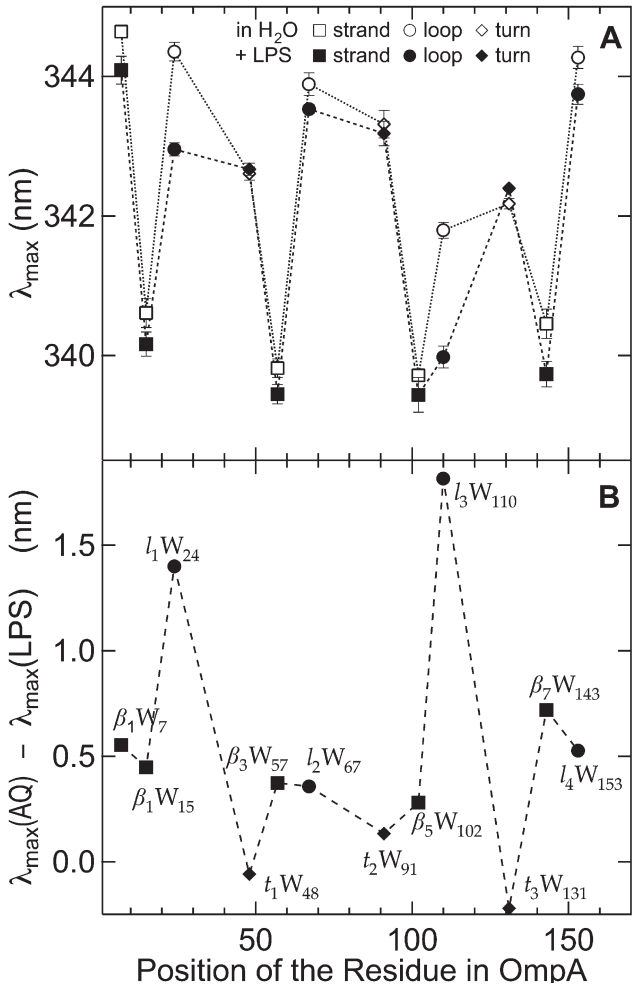

FIGURE 5: LPS binding leads to only minor changes in OmpA. (A) The emission maxima of the fluorescence spectra of the OmpA mutants in the absence, $\lambda_{max}(AQ)$ (open symbols), and in the presence (filled symbols) of a 5-fold molar excess of LPS, $\lambda_{max}(LPS)$, are plotted as a function of the tryptophan location in β-strands (□, ■) in loops (○, ●) and in turns (◇, ◆). (B) Calculated differences, $\lambda_{max}(AQ) - \lambda_{max}(LPS)$, indicate only minor changes in spectral maxima, except for loops l_1 and l_3. Fluorescence spectra were recorded immediately after LPS addition at 25 °C.

remain at the surface of water-collapsed OmpA. Shifts in λ_{max} of l_3W_{110} and t_3W_{131} were slightly larger ($\lambda_{max}(AQ) = \sim 342$ nm). Changes in λ_{max} and in the fluorescence intensities were consistent and indicated that in aqueous OmpA the β-strands are less exposed to water than the loops and the turns (Figure 4 and Table 3).

In the presence of a 4-fold molar excess of Skp (Figure 4A, filled symbols), emission maxima of all *TMD*-W_n mutants were shifted toward even shorter wavelength, with λ_{max} ranging from ~336 to ~340 nm. The relative pattern of the fluorescence data of the 13 investigated OmpA mutants remained largely unaltered across the polypeptide chain, suggesting only minor conformational changes in OmpA upon binding to Skp_3, except for the C-terminus of the *TMD*. The changes in λ_{max} were largest for l_yW_n and t_zW_n mutants carrying the tryptophan in a loop or turn. This is most obvious in a plot of the difference in λ_{max} in the presence and absence of Skp as a function of the position of the mutated residue (Figure 4B). The shifts of the fluorescence maxima, $\Delta\lambda_{max}$, indicated a strong change in the polarity of the microenvironment of the fluorescent tryptophans of OmpA upon Skp binding. This demonstrated removal of water from the entire *TMD* of OmpA by Skp, including the polar loop and turn regions. $\Delta\lambda_{max}$ of the β_xW_n decreased from the N- to the C-terminus of the *TMD*.

LPS Effect on the Single-Trp OmpA Mutants in the Absence of Skp. We previously reported that Skp facilitates folding of OmpA into lipid bilayers, when LPS is simultaneously present (*8*). We also observed LPS binding to a preformed OmpA·Skp_3 complex (*14*). This raised the question whether the interaction with LPS changes the topology of the OmpA·Skp_3 complex. To address this question, we first examined the effect of LPS on OmpA alone in aqueous solution after urea dilution. Small fluorescence increases, ranging from 2% to 15% at 330 nm, and minor decreases of λ_{max}, ranging from 0 to −1.8 nm, were observed. This is consistent with the previous report that a 5-fold molar excess of LPS increases F_{330} of wt-OmpA by ~12% (*8*). The strongest changes upon LPS binding were observed for l_1W_{24} and l_3W_{110}, for which F_{330} increased by about +10% and +15%, respectively. Figure 5 shows the λ_{max}

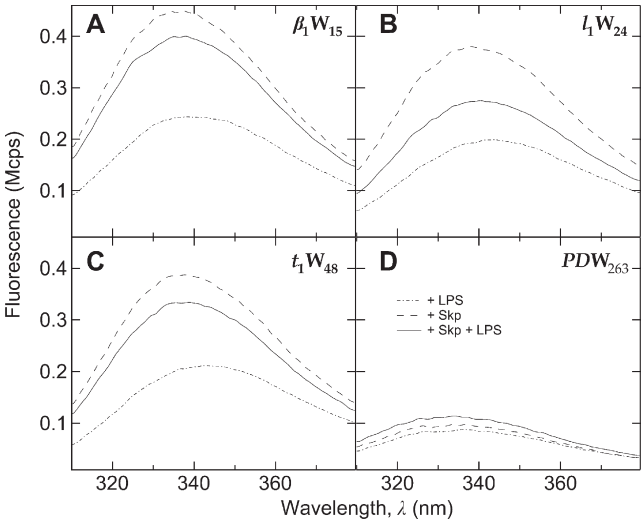

FIGURE 6: LPS binds to complexes of Skp and OmpA. The fluorescence spectra of four single-Trp mutants of OmpA, β_1W_{15} (A), l_1W_{24} (B), t_1W_{48} (C), and PDW_{263} (D) in the presence of a 5-fold molar excess of LPS (− · −), in the presence of a 4-fold molar excess of Skp (− −), and in the presence of both Skp and LPS (—), indicate that LPS binds to preformed complexes of Skp and OmpA. The concentration of each OmpA mutant was 1.15 μM. Spectra were recorded at 25 °C.

of the fluorescence of W_n-OmpA mutants in the absence and in the presence of a 5-fold molar excess of LPS. In comparison to complex formation of OmpA with Skp, addition of LPS to OmpA affected the W fluorescence spectra only slightly. The largest shifts of λ_{max} by ∼−1.5 nm were observed for l_1W_{24} and l_3W_{110}, suggesting sites for LPS interaction in outer loops l_1 and l_3 of *TMD*-OmpA. In contrast, W in turn and strand regions of OmpA indicated little or no interaction with LPS although the strands of OmpA face the fatty acyl chains of LPS in the lipid bilayer.

LPS Interacts with OmpA·Skp$_3$ Complexes in the Loop Regions of OmpA. To examine the effect of LPS on OmpA·Skp$_3$ complexes, we recorded the fluorescence spectra of β_1W_{15}, l_1W_{24}, t_1W_{48}, and PDW_{263}, each in complex with Skp either in the absence or in the presence of a 5-fold molar excess of LPS (Figure 6). Upon LPS binding to these complexes, the fluorescence intensities of β_1W_{15}, l_1W_{24}, and t_1W_{48} were decreased by −13%, −31%, and −9%, and the λ_{max} were shifted toward longer wavelength by $\Delta\lambda_{max} \approx +0.5$, $\approx +1.8$, and $\approx +0.2$ nm. To compare the effect of LPS for all W_n-OmpA·Skp$_3$ complexes, we plotted the fluorescence intensity (F_{330}) ratio of each complex in the absence and presence of LPS (Figure 7A) and the corresponding differences in the emission maxima, $\Delta\lambda_{max}$ (Figure 7B), as a function of the position of the introduced W. Mutants containing W in the TM β-strands or in the periplasmic turns of OmpA showed only small differences in fluorescence of their complexes with Skp when LPS was added. In stark contrast, fluorescence spectra of l_1W_{24}, l_2W_{67}, and l_4W_{153} indicated a much stronger effect of LPS binding to W_n-OmpA·Skp$_3$ complexes. Their fluorescence maxima were shifted by $\Delta\lambda_{max} \geq +1.8$ nm, and their fluorescence emissions at 330 nm were decreased to ∼65−70% upon LPS binding, suggesting a conformation change and exposure specifically of the loop regions l_1, l_2, and l_4 to a more polar aqueous environment while the shortest loop l_3 was less affected.

The Turn Regions of OmpA Remain Tightly Bound When LPS Is Added to OmpA·Skp$_3$ Complexes. Since

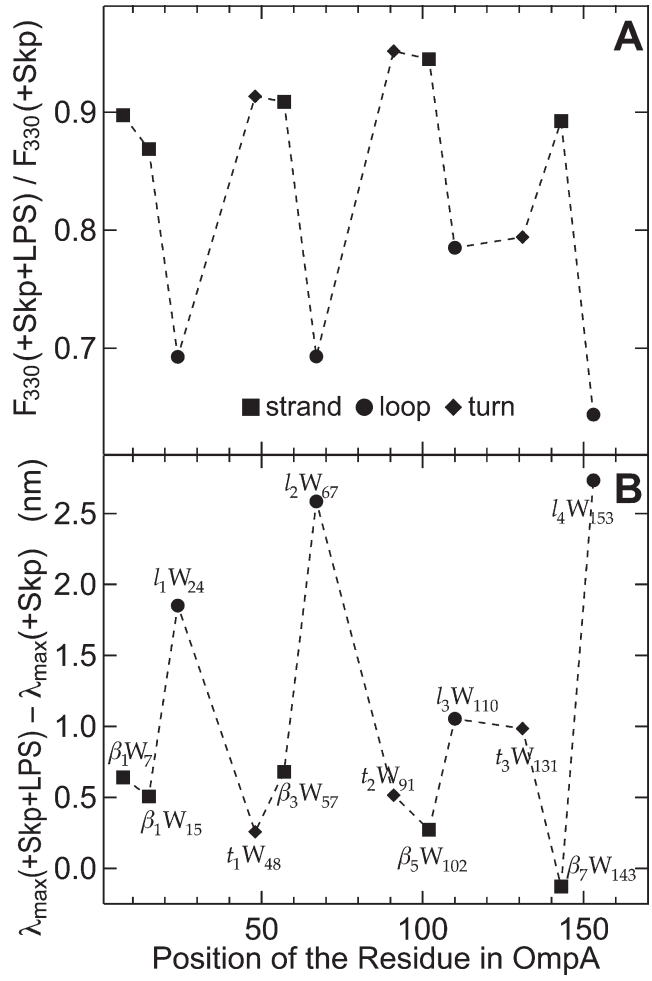

FIGURE 7: LPS binding to preformed OmpA·Skp complexes changes the environment of the outer loops of OmpA. (A) The ratio of the fluorescence intensities of the Skp·OmpA complexes in the presence and absence of LPS at 330 nm is much lower for the outer loops (●) than for the periplasmic turns (◆) and β-strands (■), indicating a more polar environment of the loops upon LPS binding to Skp·OmpA complexes. (B) Correspondingly, the difference of the wavelength of the fluorescence emission maxima of the complex in the absence and in the presence of LPS, $\Delta\lambda_{max}$, shows the largest shifts for loops l_1, l_2, and l_3.

previous work demonstrated that OmpA folds faster in the presence of both Skp and LPS than in the presence of Skp alone (*8*), it is interesting to compare the combined effect of Skp and LPS in complexes with OmpA to the water-collapsed form of OmpA. Fluorescence intensity ratios and emission maxima shifts obtained from the corresponding spectra of the W_n-OmpA mutants are shown in Figure 8 as a function of the position of the W in the polypeptide chain. Fluorescence spectra of the t_zW_n mutants displayed the largest changes, with $\Delta\lambda_{max}$ ranging from 3.7 to 4.5 nm and the largest increase in their relative fluorescence increased between 66% and 86%. In comparison, fluorescence emissions of β_xW_n and l_yW_n mutants, containing W in strands or loops, were less affected. The data showed that periplasmic turns of OmpA remain bound to Skp in a less polar environment even in the presence of LPS, while loop regions of the *TMD* are exposed to a more polar environment when LPS is added. Only Ws placed into the N-terminal first β-strand and first outer loop displayed stronger changes in the presence of both Skp and LPS, with $\Delta\lambda_{max}$ ranging from ∼3.8 to ∼4.2 nm. The influence of both LPS and Skp on the wavelength of the fluorescence maxima of

Downloaded by UNIV KONSTANZ on November 5, 2009 | http://pubs.acs.org
Publication Date (Web): April 21, 2009 | doi: 10.1021/bi9004039

Downloaded by UNIV KONSTANZ on November 5, 2009 | http://pubs.acs.org
Publication Date (Web): April 21, 2009 | doi: 10.1021/bi9004039

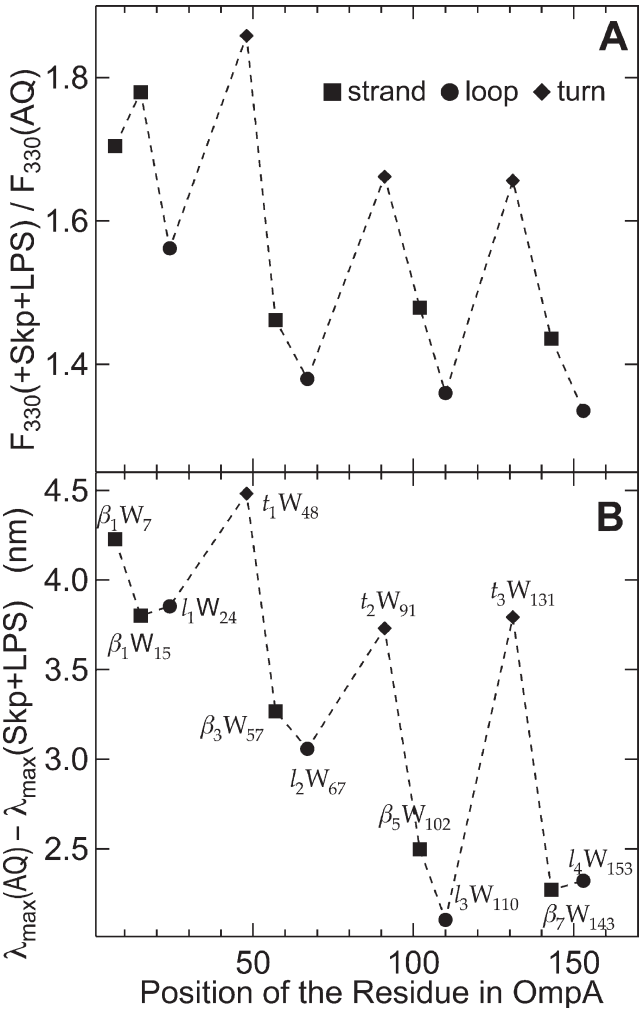

FIGURE 8: In OmpA/Skp/LPS complexes, periplasmic turns are most strongly bound in comparison with strand and loop regions. (A) Fluorescence intensity ratios at 330 nm and (B) differences in λ_{max} of W_n mutants in the presence of both Skp and LPS and in the absence of Skp and LPS in aqueous form are shown as a function of the location of the single tryptophan in strands (■), loops (●), and turns (◆). The fluorescence intensity increases and shifts in the wavelengths of the emission maxima are most pronounced for the N-terminal region of OmpA, but also observed closer to the C-terminus of the transmembrane domain.

β_xW_n and l_yW_n mutants gradually decreased from the N-terminus to the C-terminus. At the C-terminus, $\Delta\lambda_{max}$ was only ≈2.3 nm for β_7W_{143} and l_4W_{153}, i.e., about half the $\Delta\lambda_{max}$ observed for the periplasmic turns. Similarly, fluorescence ratios F_{330}(+Skp + LPS)/F_{330}(AQ) exceeded +60% for the t_zW_n mutants but were much lower, i.e., ≈ +33% to +45%, for β_3W_{57}, l_2W_{67}, β_5W_{102}, l_3W_{110}, β_7W_{143}, and l_4W_{153}. These results suggest that binding of Skp/LPS to OmpA is weaker toward the C-terminus, except for the periplasmic turns of OmpA.

A comparison of the data sets in Figures 4B and 8B shows that the l_yW_n in the long and flexible loops display a change toward a more polar environment upon addition of LPS to Skp-bound OmpA. In contrast, the polarity of the environment of the t_zW_n in the periplasmic turns changes very little, indicating that turns remain associated with Skp even when LPS is added. Both conformation and orientation of Skp-bound OmpA therefore change after binding of LPS, exposing the loops of OmpA to a more polar environment. This change in orientation of OmpA correlates well with the observed effect of LPS to facilitate insertion and folding of OmpA from its complex with Skp (*8*), which already suggested that the stability of the OmpA·Skp complex is weakened in the presence of LPS.

Intramolecular Site-Directed Tryptophan Fluorescence Quenching Indicates That OmpA Only Folds after Insertion into Lipid Bilayers. To explore formation of structure in OmpA upon binding to Skp, we used intramolecular fluorescence quenching. Tryptophan fluorescence quenching by nitroxyl spin-labels is distance dependent (*26*, *27*) and can be used to monitor protein folding for single-tryptophan, single-cysteine mutants that are nitroxyl spin-labeled at the C (*28*). We therefore prepared a second set of OmpA mutants, based on plasmids used for expression of several *TMD* W_n mutants. The plasmids were used to introduce a single-C residue on the DNA level for expression of single-W/single-C mutants, W_nC_m, and subsequent site-directed spin-labeling of the sulfhydryl-reactive C. The replaced residue was selected based on the structure of OmpA (PDB entry 1BXW) and was in a direct neighbor strand in close proximity to the W, also facing the outer surface of the OmpA barrel (Figure 1). Five such W_nC_m mutants were prepared (Table 1B). For reference, spectra were also recorded for all mutants in the absence of the spin-label under otherwise identical conditions. To avoid unwanted disulfide dimerization of the non-spin-labeled mutants, the Cs were methylated. Both methylated and spin-labeled forms of all mutants were completely folded when incubated with preformed DOPC bilayers, as judged by cold SDS−PAGE.

To monitor the degree of folding of OmpA in 8 M urea, in water, in complex with either Skp or LPS or both, and in lipid bilayers, we recorded the fluorescence spectra of spin-labeled or methylated W_nC_m mutants. The fluorescence spectra of $W_{15}C_{162}$ in 8 M urea, in aqueous buffer, and in the presence of either LPS or Skp or both Skp and LPS are shown in Figure 9. There was no difference between the fluorescence intensities at 330 nm (F_{330}) of the S-methylated or spin-labeled forms of the $W_{15}C_{162}$ mutant, indicating that residues W_{15} and C_{162} (see Figure 1) were not in close proximity under these conditions. However, when spin-labeled $W_{15}C_{162}$ was incubated with preformed DOPC bilayers, the fluorescence intensity of the S-methylated $W_{15}C_{162}$ mutant was twice as large as the intensity of the spin-labeled $W_{15}C_{162}$ mutant (Figure 9C,D). The same observation was made for the mutants W_7C_{43}, W_7C_{170}, $W_{15}C_{35}$, $W_{15}C_{162}$, and $W_{57}C_{35}$ (Figure 10). These data indicated that the entire β-barrel domain remains unfolded in water and in complex with Skp, with LPS, or with Skp and LPS. Folding of the β-barrel domain required the incubation with a preformed lipid bilayer.

DISCUSSION

In the present study we describe structural properties of aqueous and Skp-bound forms of OmpA, either in the absence or in the presence of negatively charged LPS in unprecedented detail. Several new observations were made. First, tryptophan fluorescence spectroscopy demonstrated that, in the water-collapsed form of OmpA, residues of the hydrophobic transmembrane strand regions are more shielded against polar interactions with water than residues of the periplasmic turns and outer loops, which are more surface exposed. Second, Skp_3 binds to the entire transmembrane domain of OmpA, and this binding is asymmetric. Skp binding has a stronger effect on the N-terminus than on the C-terminus of the *TMD* of OmpA (Figure 4). Third, binding is also asymmetric toward loop, turn,

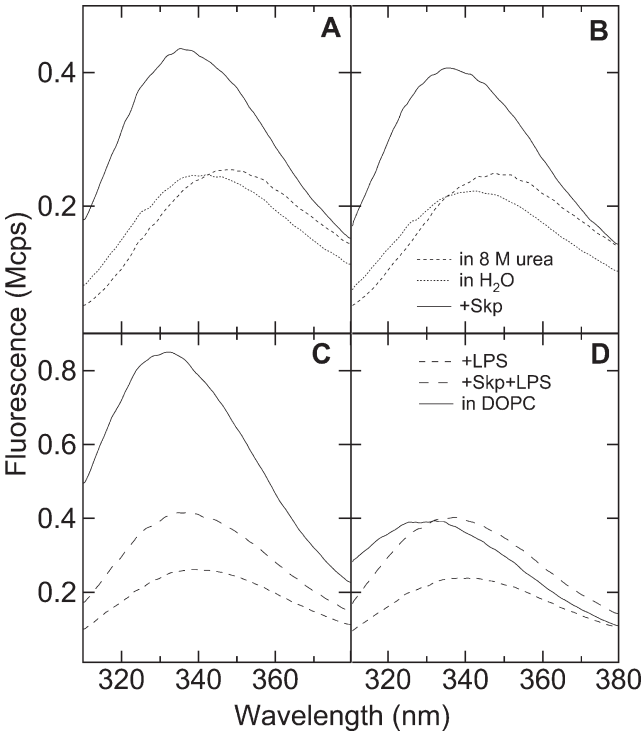

FIGURE 9: OmpA remains unfolded in complex with Skp and LPS. Proximity of the single-Trp and the single-Cys residue in the mutant $W_{15}C_{162}$ was tested by intramolecular fluorescence quenching via a cysteine-linked spin-label. (A, C) Spectra of the S-methylated and (B, D) spectra of the spin-labeled $W_{15}C_{162}$ OmpA mutant. Panels A (methylated form) and B (spin-labeled form) show the fluorescence spectra in 8 M urea (- - -), after 100-fold urea dilution in Tris buffer (10 mM, pH 8) (· · ·), and in the presence of a 4-fold molar excess of Skp (—). Panels C (methylated form) and D (spin-labeled form) show spectra in the presence of LPS (- - -), Skp and LPS (— —), and after incubation with lipid bilayers of DOPC (—). Only when folded into DOPC bilayers is fluorescence of spin-labeled $W_{15}C_{162}$ quenched compared to the S-methylated mutant.

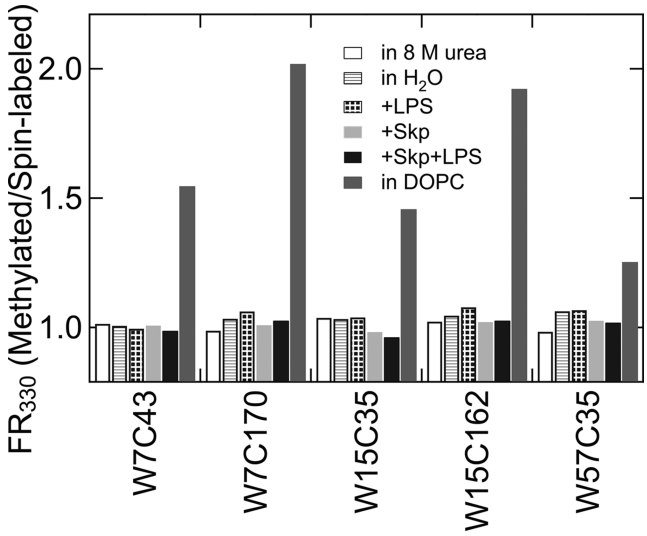

FIGURE 10: Skp and LPS do not induce native-like formation of antiparallel β-strands. Structure formation in the transmembrane domain of OmpA was probed as described in the legend to Figure 8 for four additional W_nC_m mutants, namely, W_7C_{43}, W_7C_{170}, $W_{15}C_{35}$, and $W_{57}C_{35}$. The fluorescence intensity ratios of each mutant in methylated and in quencher-labeled form in 8 M urea, in Tris buffer (10 mM, pH 8), in the presence of a 5-fold molar excess of LPS, a 4-fold molar excess of Skp, and in the presence of both LPS and Skp, and finally after folding into DOPC bilayers indicate formation of native antiparallel β-sheet structure only in lipid bilayers.

and strand regions of the *TMD* of OmpA. Fluorescence data indicated that the polar loops and turns of OmpA are more affected by Skp binding than the hydrophobic β-strand regions. Fourth, LPS binding to OmpA·Skp_3 complexes displaces the loops of OmpA from the Skp surface, exposing them to the aqueous solution. In this ternary complex, the periplasmic turns of OmpA remain tightly bound, indicating that LPS alters the topology of OmpA in the ternary complex and facilitates a change in OmpA orientation, preparing it for the more efficient membrane insertion reported in kinetic studies with wt-OmpA (*8*). Fifth, intramolecular site-directed fluorescence quenching revealed that the β-barrel domain does not fold in the presence of Skp, as also shown previously by circular dichroism spectroscopy (*8*) and in a recent NMR study (*29*). Finally, sixth, we observed that native tertiary contacts are not formed when Skp and LPS are both present. Instead, OmpA strictly requires the presence of lipid bilayers for folding (Figure 10).

OmpA Strand Regions Form an Unstructured Outside-In Conformation in the Aqueous Intermediate. Our site-directed fluorescence data of 12 different W_n-OmpA mutants indicated a partially "outside-in" conformation of the β-strand regions of the aqueous form of OmpA. The tryptophans of the more hydrophobic β-strand regions, which face the lipid acyl chains in the membrane-inserted folded form, were oriented more toward the inside of the water-collapsed form of OmpA, while the loop and turn regions formed the surface. This reduces OmpA aggregation in aqueous solution and is consistent with a previous circular dichroism study, which indicated that most of the amphipathic β-sheet secondary structure of the *TMD* forms upon membrane insertion (*30*). A lack of native structure in the *TMD* of OmpA was also observed when aqueous OmpA formed complexes with Skp (Figure 10), consistent with recent NMR data (*29*), and when five LPS were added to one OmpA·Skp_3 complex (Figure 10). The *TMD* of OmpA only folded when complexes of unfolded OmpA, Skp, and LPS were exposed to lipid membranes. The relative fluorescence changes along the polypeptide chain were quite similar for the water-collapsed form of OmpA and for its Skp-bound form (Figure 4A), while the fluorescence changes upon Skp binding were greater for Ws in the loops and turns than for Ws in the strands (Figure 4B). Therefore, it seems likely that reversal of the partially outside-in conformation of aqueous OmpA does not take place upon complex formation of OmpA with Skp. Instead, the formation of a continuous hydrophobic surface and folding of OmpA is initiated at the membrane−water interface and coupled to integration into the hydrophobic core of the membrane (Figure 10).

Skp Interacts Asymmetrically with N- and C-Terminal Strand Regions of the TMD *of OmpA*. Tryptophans introduced into turns or loops that were surface-exposed in the aqueous forms showed stronger changes in fluorescence due to Skp binding than tryptophans in the β-strand regions (Figure 4B), indicating water removal from the OmpA surface, in particular from the loops and turns but also from the more hydrophobic β-strands. In context with our previous study, which showed that OmpA binding to Skp depends on the pH and on the ionic strength (*14*), our present site-directed fluorescence results indicate that polar or electrostatic interactions between loops or turns of OmpA (p*I* ~5.5) and polar or charged residues of the highly basic Skp (p*I* ~10.5) are major determinants for Skp binding to OmpA. The loops l_1, l_2, and l_4 and the turns t_2 and t_3 contain negatively charged residues that may bind

Downloaded by UNIV KONSTANZ on November 5, 2009 | http://pubs.acs.org
Publication Date (Web): April 21, 2009 | doi: 10.1021/bi9004039

to Skp, which contains positively charged residues all over its tentacle domain, in particular in the tip region of the tentacles (*11*, *12*, *14*). β-Turn regions containing a negative net charge are quite common in outer membrane proteins of Gram-negative bacteria and found, e.g., in OmpA, OmpG, OmpW, OmpT, FadL, OmpF, LamB, and FhuA of *E. coli* but also in NalP and NspA of *N. meningitidis*. The interaction of Skp with the *TMD* of OmpA is asymmetric regarding OmpA, since Skp dehydrates strand regions closer to the N-terminus of OmpA more strongly than the C-terminal strands. In OmpA·Skp_3 complexes, this asymmetry is not observed for the periplasmic turns and outer loops of OmpA, which bound similarly to the C- and N-termini of the *TMD* (Figure 4B).

LPS Binding Changes the Asymmetry of Skp·OmpA Interactions and Exposes the Outer Loops of OmpA to a More Polar Environment. When LPS was added to Skp·OmpA complexes, the asymmetry previously observed only for the strand regions (Figure 4) was then also observed for the loop regions (Figure 8B), indicating a change in the polarity of the environment of the loops, in particular in the C-terminal half of the *TMD* of OmpA. A comparison of Figures 4B, 5B, and 8B suggests that LPS binding to OmpA·Skp_3 complexes reduces the shielding of the loops of OmpA against interactions with water (Figures 4B and 8B). The reduction is strongest at the C-terminus of the *TMD*. However, the fluorescence properties of t_1W_{48}, t_2W_{91}, and t_3W_{131} remain largely unaltered upon LPS addition, indicating tight binding of the turns to Skp_3 even when LPS is added (Figures 4B and 8B). These results suggest that binding of negatively charged LPS leads to a partial release of the negatively charged *TMD* of OmpA from the complex with the positively charged Skp, which remains bound mostly to the turn regions of OmpA and to the N-terminus of the *TMD*. This interpretation is consistent with our previous study (*14*), which demonstrated that the tryptophans of wt-OmpA, all located in transmembrane β-strands (but close to the loops), become more accessible to the aqueous fluorescence quencher acrylamide when LPS is added to Skp_3·OmpA complexes. This might be caused by the partial release of loop regions of the *TMD* of OmpA from the complex with Skp due to interactions of the complex with LPS.

Electrostatic Interactions Dominate over Hydrophobic Interactions Regarding Complex Formation of Skp with OMPs. Figure 11 summarizes tentative models for OmpA complexes with Skp and with Skp and LPS. Our data demonstrate that unfolded OmpA (A) develops an outside-in conformation in aqueous solution (B) after urea dilution. Aqueous OmpA is bound by the chaperone Skp via multiple polar and also hydrophobic interactions of its entire TM domain, including all strands, turns, and loops (C). We recently showed that electrostatic interactions between OmpA and Skp are important for complex formation. The binding constant was reduced at an increased ionic strength, and binding was not observed at pH values close to the isoelectric points of either Skp or OmpA (*14*). This was not expected since the hydrophobic nature of transmembrane proteins and their tendency to aggregate in aqueous solution suggested that hydrophobic interactions should dominate the binding of a TMP to a chaperone. However, OMPs form pores through the membrane, and the transmembrane strands therefore have a highly amphipathic nature in folded form. The unfolded or collapsed OMPs may not present enough continuous hydrophobic surface area to bind chaperones via hydrophobic interactions alone. Binding of negatively charged LPS to OmpA·Skp_3

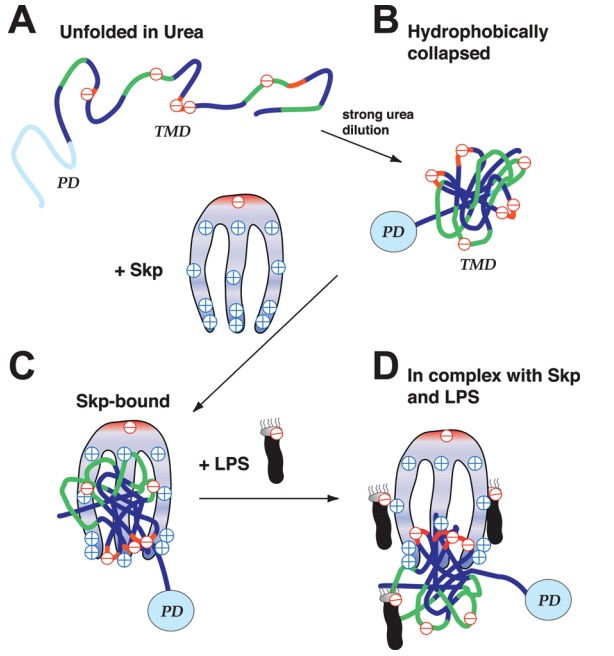

FIGURE 11: Scheme for the interaction of OmpA with Skp and LPS. (A) Unfolded OmpA in 8 M urea forms a random coil structure. The dark blue lines represent the transmembrane strand regions of the OmpA polypeptide chain, the green lines the polar loop, and the red lines the polar turn regions. The periplasmic domain is colored in light blue. Overall, OmpA is negatively charged above p*I* ~5.5, e.g., in the turn regions, indicated by (−). (B) The transmembrane domain of OmpA forms a water-soluble intermediate state in water while the soluble periplasmic domain folds. (C) The positively charged Skp tentacles (+) bind the entire transmembrane domain of OmpA through multiple electrostatic and also hydrophobic interactions. (D) Negatively charged LPS binds to OmpA·Skp_3 complexes, leading to a partial release of OmpA from the complex. The turn regions of OmpA remain bound to Skp_3. This leads to a reorientation of OmpA and might explain the observed LPS-facilitated folding of wt-OmpA into lipid bilayers in kinetic experiments (*8*) since the conformation of OmpA in the complex is changed.

complexes results in a partial release of the outer loops of OmpA from Skp_3, which likely leads to a reorientation of OmpA (D). The relatively small amount of five LPS per OmpA·Skp_3 complex that was added in aqueous solution was insufficient to form a hydrophobic environment for OmpA folding. However, binding of five LPS to the OmpA·Skp_3 complex is known to result in a partial exposure of the Ws in the β-strands of OmpA to the aqueous environment (*14*) and to facilitate membrane insertion (*8*).

Interestingly, Omp85 (YaeT) of *E. coli*, which is the receptor for OMP assembly into the outer membrane, is composed of a membrane-inserted C-terminal half and an N-terminal periplasmic half. The periplasmic domain carries a negative net charge and may serve as a docking site for positively charged Skp with bound OMPs. The N-terminal domain might assume the role of negatively charged LPS in weakening the interactions of Skp with bound OMPs.

Skp and SurA Display Different Modes of OMP Binding to Periplasmic Chaperones. Trimeric Skp binds to the *TMD* but not to the *PD* of unfolded OmpA with nanomolar affinity (*14*) and forms stable 1:1 complexes (*8*, *14*). Here we observed that Skp does not recognize isolated regions of the *TMD* but instead binds the entire *TMD*-OmpA. The fluorescence data also indicate that there is no specific motif in the β-strand regions of the *TMD* of OmpA that is preferentially recognized by Skp. Another

Downloaded by UNIV KONSTANZ on November 5, 2009 | http://pubs.acs.org
Publication Date (Web): April 21, 2009 | doi: 10.1021/bi9004039

periplasmic chaperone, SurA, has been reported to specifically recognize and bind the peptide sequence *Ar-Rnd-Ar*, where *Ar* is an aromatic and *Rnd* any amino acid (*31*−*33*). Although the tryptophans β_3W_{57} and β_7W_{143} present in OmpA are part of such a motif (Figure 1), the fluorescence data obtained in this study do not suggest any preferred sequences in OmpA for Skp binding. However, the periplasmic turns of OmpA might still be an exception since they are bound stronger to Skp than loops and strands. The affinity of SurA for OMPs is in the micromolar range (*32*), while Skp binds with nanomolar affinity (*8*, *14*), indicating that the modes of binding are very different for these two chaperones. A likely explanation for the high affinity of Skp for unfolded OMPs is its binding to the entire unfolded transmembrane domain and not just a short stretch of amino acids as reported for SurA (*31*−*33*).

REFERENCES

1. Chen, R., and Henning, U. (1996) A periplasmic protein (Skp) of *Escherichia coli* selectively binds a class of outer membrane proteins. *Mol. Microbiol. 19*, 1287–1294.
2. Schäfer, U., Beck, K., and Müller, M. (1999) Skp, a molecular chaperone of gram-negative bacteria, is required for the formation of soluble periplasmic intermediates of outer membrane proteins. *J. Biol. Chem. 274*, 24567–24574.
3. Rouvière, P. E., and Gross, C. A. (1996) SurA, a periplasmic protein with peptidyl-prolyl isomerase activity, participates in the assembly of outer membrane porins. *Genes Dev. 10*, 3170–3182.
4. Lazar, S. W., and Kolter, R. (1996) SurA assists the folding of *Escherichia coli* outer membrane proteins. *J. Bacteriol. 178*, 1770–1773.
5. Kleinschmidt, J. H. (2007) Assembly of integral membrane proteins from the periplasm into the outer membrane, in *The Periplasm* (Ehrmann, M., Ed.) pp 30−66, ASM Press, Herndon, VA.
6. Rizzitello, A. E., Harper, J. R., and Silhavy, T. J. (2001) Genetic evidence for parallel pathways of chaperone activity in the periplasm of *Escherichia coli*. *J. Bacteriol. 183*, 6794–6800.
7. Behrens, S., Maier, R., de Cock, H., Schmid, F. X., and Gross C. A. (2001) The SurA periplasmic PPIase lacking its parvulin domains functions in vivo and has chaperone activity. *EMBO J. 20*, 285–294.
8. Bulieris, P. V., Behrens, S., Holst, O., and Kleinschmidt, J. H. (2003) Folding and insertion of the outer membrane protein OmpA is assisted by the chaperone Skp and by lipopolysaccharide. *J. Biol. Chem. 278*, 9092–9099.
9. Harms, N., Koningstein, G., Dontje, W., Müller, M., Oudega, B., Luirink, J., and de Cock, H. (2001) The early interaction of the outer membrane protein phoe with the periplasmic chaperone Skp occurs at the cytoplasmic membrane. *J. Biol. Chem. 276*, 18804–18811.
10. Jarchow, S., Luck, C., Gorg, A., and Skerra, A. (2008) Identification of potential substrate proteins for the periplasmic *Escherichia coli* chaperone Skp. *Proteomics 8*, 4987–4994.
11. Korndörfer, I. P., Dommel, M. K., and Skerra, A. (2004) Structure of the periplasmic chaperone Skp suggests functional similarity with cytosolic chaperones despite differing architecture. *Nat. Struct. Mol. Biol. 11*, 1015–1020.
12. Walton, T. A., and Sousa, M. C. (2004) Crystal structure of Skp, a prefoldin-like chaperone that protects soluble and membrane proteins from aggregation. *Mol. Cell 15*, 367–374.
13. Schlapschy, M., Dommel, M. K., Hadian, K., Fogarasi, M., Korndörfer, I. P., and Skerra, A. (2004) The periplasmic *E. coli* chaperone Skp is a trimer in solution: biophysical and preliminary crystallographic characterization. *Biol. Chem. 385*, 137–143.
14. Qu, J., Mayer, C., Behrens, S., Holst, O., and Kleinschmidt, J. H. (2007) The trimeric periplasmic chaperone Skp of *Escherichia coli* forms 1:1 complexes with outer membrane proteins via hydrophobic and electrostatic interactions. *J. Mol. Biol. 374*, 91–105.
15. Prilipov, A., Phale, P. S., Van Gelder, P., Rosenbusch, J. P., and Koebnik, R. (1998) Coupling site-directed mutagenesis with high-level expression: large scale production of mutant porins from *E. coli*. *FEMS Microbiol. Lett. 163*, 65–72.
16. Kleinschmidt, J. H., den Blaauwen, T., Driessen, A., and Tamm, L. K. (1999) Outer membrane protein A of *E. coli* inserts and folds into lipid bilayers by a concerted mechanism. *Biochemistry 38*, 5006–5016.
17. Surrey, T., and Jähnig, F. (1992) Refolding and oriented insertion of a membrane protein into a lipid bilayer. *Proc. Natl. Acad. Sci. U.S.A. 89*, 7457–7461.
18. Hunziker, P. E. (1991) Cysteine modification of metallothionein. *Methods Enzymol. 205*, 399–400.
19. Berliner, L. J., Grunwald, J., Hankovszky, H. O., and Hideg, K. (1982) A novel reversible thiol-specific spin label: papain active site labeling and inhibition. *Anal. Biochem. 119*, 450–455.
20. Riddles, P. W., Blakeley, R. L., and Zerner, B. (1983) Reassessment of Ellman's reagent. *Methods Enzymol. 91*, 49–60.
21. Vinogradov, E. V., Van Der Drift, K., Thomas-Oates, J. E., Meshkov, S., Brade, H., and Holst, O. (1999) The structures of the carbohydrate backbones of the lipopolysaccharides from *Escherichia coli* rough mutants F470 (R1 core type) and F576 (R2 core type). *Eur. J. Biochem. 261*, 629–639.
22. Müller-Loennies, S., Holst, O., and Brade, H. (1994) Chemical structure of the core region of *Escherichia coli* J-5 lipopolysaccharide. *Eur. J. Biochem. 224*, 751–760.
23. Ladokhin, A. S., and Holloway, P. W. (1995) Fluorescence of membrane-bound tryptophan octyl ester: a model for studying intrinsic fluorescence of protein-membrane interactions. *Biophys. J. 69*, 506–517.
24. Arora, A., Rinehart, D., Szabo, G., and Tamm, L. K. (2000) Refolded outer membrane protein A of *Escherichia coli* forms ion channels with two conductance states in planar lipid bilayers. *J. Biol. Chem. 275*, 1594–1600.
25. Kleinschmidt, J. H. (2006) Folding kinetics of the outer membrane proteins OmpA and FomA into phospholipid bilayers. *Chem. Phys. Lipids 141*, 30–47.
26. Chattopadhyay, A., and London, E. (1987) Parallax method for direct measurement of membrane penetration depth utilizing fluorescence quenching by spin-labeled phospholipids. *Biochemistry 26*, 39–45.
27. London, E., and Feigenson, G. W. (1981) Fluorescence quenching in model membranes. 1. Characterization of quenching caused by a spin-labeled phospholipid. *Biochemistry 20*, 1932–1938.
28. Anbazhagan, V., Qu, J., Kleinschmidt, J. H., and Marsh, D. (2008) Incorporation of outer membrane protein OmpG in lipid membranes. Protein-lipid interactions and β-barrel orientation. *Biochemistry 47*, 6189–6198.
29. Walton, T. A., Sandoval, C. M., Fowler, C. A., Pardi, A., and Sousa, M. C. (2009) The cavity-chaperone Skp protects its substrate from aggregation but allows independent folding of substrate domains. *Proc. Natl. Acad. Sci. U.S.A. 106*, 1772–1777.
30. Kleinschmidt, J. H., and Tamm, L. K. (2002) Secondary and tertiary structure formation of the β-barrel membrane protein OmpA is synchronized and depends on membrane thickness. *J. Mol. Biol. 324*, 319–330.
31. Bitto, E., and McKay, D. B. (2003) The periplasmic molecular chaperone protein SurA binds a peptide motif that is characteristic of integral outer membrane proteins. *J. Biol. Chem. 278*, 49316–49322.
32. Bitto, E., and McKay, D. B. (2004) Binding of phage-display-selected peptides to the periplasmic chaperone protein SurA mimics binding of unfolded outer membrane proteins. *FEBS Lett. 568*, 94–98.
33. Hennecke, G., Nolte, J., Volkmer-Engert, R., Schneider-Mergener, J., and Behrens, S. (2005) The periplasmic chaperone SurA exploits two features characteristic of integral outer membrane proteins for selective substrate recognition. *J. Biol. Chem. 280*, 23540–23548.
34. Vogel, H., and Jähnig, F. (1986) Models for the structure of outer-membrane proteins of *Escherichia coli* derived from Raman spectroscopy and prediction methods. *J. Mol. Biol. 190*, 191–199.
35. Dornmair, K., Kiefer, H., and Jähnig, F. (1990) Refolding of an integral membrane protein. OmpA of *Escherichia coli*. *J. Biol. Chem. 265*, 18907–18911.
36. Schweizer, M., Hindennach, I., Garten, W., and Henning, U. (1978) Major proteins of the *Escherichia coli* outer cell envelope membrane. Interaction of protein II with lipopolysaccharide. *Eur. J. Biochem. 82*, 211–217.
37. Pocanschi, C. L., Dahmane, T., Gohon, Y., Rappaport, F., Apell, H.-J., Kleinschmidt, J. H., and Popot, J.-L. (2006) Amphipathic polymers: tools to fold integral membrane proteins to their active form. *Biochemistry 45*, 13954–13961.

Downloaded by UNIV KONSTANZ on November 5, 2009 | http://pubs.acs.org
Publication Date (Web): April 21, 2009 | doi: 10.1021/bi9004039